

Emergent regularities and scaling in armed conflict data

Edward D. Lee,¹ Bryan C. Daniels,^{2,3} Christopher R. Myers,^{1,4} David C. Krakauer,² Jessica C. Flack²

¹Department of Physics, 142 Sciences Dr, Cornell University, Ithaca NY 14853

²Santa Fe Institute, 1399 Hyde Park Rd, Santa Fe, NM 87501

³ASU-SFI Center for Biosocial Complex Systems, Arizona State University, Tempe, AZ 85287

⁴Center for Advanced Computing, Cornell University, Ithaca, NY 14853

(Dated: June 3, 2022)

Large-scale armed conflict is a characteristic feature of modern societies. The statistics of conflict show remarkable regularities like power law distributions of fatalities and duration, but lack a unifying framework. We explore a large, detailed data set of 10^5 armed conflict reports spanning 20 years across nearly 10^4 kilometers. By systematically clustering spatiotemporally proximate events into *conflict avalanches*, we show that the number of conflict reports, fatalities, duration, and geographic extent satisfy consistent power law scaling relations. The temporal evolution of conflicts measured by these scaling variables display emergent symmetry, collapsing onto a universal dynamical profile over a range of scales. The measured exponents and dynamical profiles describe a system distinct from prevailing explanations of conflict growth such as forest fire models. Our findings suggest that armed conflicts are dominated by a low-dimensional process that scales with physical dimensions in a surprisingly unified and predictable way.

In the 1940s, Richardson famously noted that the distribution of fatalities in warfare followed a power law [1]. Since then, power law statistics in armed conflict have been observed across a variety of data sets including terrorism and conventional warfare [2–5]. These regularities have sparked discussion about mechanisms that would generate such patterns including cellular-automaton [6], coalescence-fragmentation [7], and self-organized critical forest fire models [8]. More broadly, self-similarity is a feature of a critical point in renormalization group theory, a framework for organizing many microscopic mechanisms into universality classes distinguished by their macroscopic properties [9, 10]. Renormalization group analysis of nonequilibrium critical phenomena explains why at large scales a low-dimensional description emerges, leading to a rich array of predictions including consistent scaling relations, universal scaling functions, and universal temporal profiles [11]. These properties suggest a self-consistent scaling framework that we show captures large-scale patterns in the statistics of armed conflict.

The central idea behind the renormalization group is the coarse-graining of a length scale that defines a mapping operation from one model to another. Thus, the coarse-graining operation describes a flow in the space of models that eventually leads to a fixed point, where separation of length scales leads to the emergence of characteristic, long-wavelength properties. Separating the basins of stable fixed points, or phases, are the critical manifolds corresponding to phase transitions. These correspond to unstable fixed points where the system becomes scale-invariant and the resulting power laws are described by a set of critical exponents. In principle, critical behavior is defined in the thermodynamic limit but real systems are finite, measurements are noisy, and systematic corrections like finite-size effects are unavoidable [12, 13]. Yet when we are close enough to a fixed point,

we expect that a few relevant scaling variables dominate and a simple description of the system emerges that is independent of many microscopic details [11]. Such a prediction presents a simple scaling hypothesis that we test with armed conflict data.

We investigate data collected in the Armed Conflict Location & Event Data Project (ACLED) that aggregates events reported by news media and regional contacts from 1997–2016 [14]. The part of the data set on Africa is notable for its extent—covering two decades,



FIG. 1. Battle avalanches in Africa between 1997–2016 [14]. Spatial distribution of largest 10 conflict avalanches by size S for given separation scales $b = 140$ km and $a = 128$ days. Spatial density is highly non-uniform, largely confined to land, and typically denser near population centers.

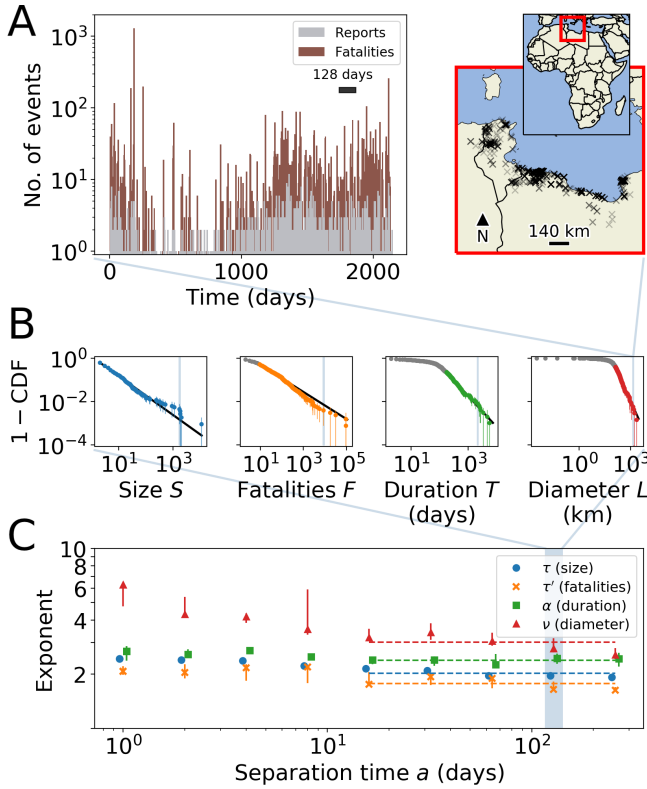


FIG. 2. (A) A single conflict avalanche erupting across Tunisia and Libya from Feb. 2, 2011 til Dec. 27, 2016 with temporal profile on left and spatial distribution on right. This avalanche consists of $S = 1,717$ reports, $F = 8,569$ fatalities, lasts $T = 2,141$ days, and extends 1,364 km as highlighted in each graph in B in blue. (B) Complementary cumulative distribution functions for avalanche scaling variables given $a = 128$ days. Points below the lower cutoff in gray. Black lines indicate maximum likelihood fits, and error bars represent 90% bootstrapped confidence intervals. The data are statistically indistinguishable from power laws at the $p \geq 0.1$ significance level (SI Section C) [18]. (C) Exponents as a function of the separation time a . Dashed lines show the average exponent value for the last five points $16 \leq a \leq 256$ days.

thousands of kilometers, and $> 10^5$ events. We analyze three kinds of events in the data set: Battles involving two or more armed groups ($K = 42,738$), Violence Against Civilians in which armed groups attack the population ($K = 39,127$), and Riots/Protests ($K = 37,582$). Each identified event has a geographic coordinate, date, and number of fatalities. Like the canonical avalanche picture for nonequilibrium critical phenomena, we call clusters of events *conflict avalanches*. Although we consider all three conflict types, we focus on the Battles (see SI for other event types).

We cluster events into conflict avalanches by setting a separation length b and separation time a such that events that are within the specified distance and time are grouped into the same avalanche (SI Section B), a procedure analogous to that done for neural avalanches

[15–17]. As we vary these scales, the typical duration and geospatial extent of conflict avalanches change systematically, but for a large range of scales the observed statistics are remarkably consistent. For the following, we fix $b = 140$ km because it is sufficiently large that conflicts can percolate through a large network while sufficiently small that the system boundaries defined by geographic features (e.g. Sahara Desert, coastlines) do not significantly impact scaling (SI Section B). In Fig. 1, we show the spatial distribution for the 10 largest avalanches by size for $b = 140$ km and $a = 128$ days. A single example of a conflict avalanche spanning Libya and Tunisia lasting over 10^3 days with nearly 10^4 reported fatalities appears in Fig. 2A along with its temporal profile. Thus, every conflict avalanche has a duration T in days, size measured by the number localized events or reports S , reported fatalities F , and geographic extent L in kilometers given by the maximally distant pair of events. This clustering operation, with only straightforward dependence on physical scales, defines a systematic way of constructing related sets of events, in contrast with notions of “battles” or “wars” which can depend on sociopolitical nuances.

As visible in Figs. 1 and 2A, the spatial density of conflict is strongly nonuniform. Large conflicts tend to concentrate along high population areas: few occur in the Sahara Desert and only a handful are reported in the oceans. Conflict density also depends on other factors like the geography of country borders (e.g. Darfur). Not only do these geopolitical features impose boundaries on the propagation of conflict, but communication technology may render physical distance irrelevant for coordinated events. Considering the effects of strong spatial nonuniformity, pinning on geographic boundaries, and rapid long distance communication—analogous to effects that destroy scaling in physical systems—it would be surprising if the length scale L fit into a scaling description.

Since such effects are less relevant for time, we choose our scaling variable as the duration of avalanches T . Then, our scaling hypothesis predicts

$$S \sim T^{ds/z}, \quad (1)$$

$$F \sim T^{d_F/z}, \quad (2)$$

and if including geographic extent L

$$L \sim T^{1/z} \quad (3)$$

with dynamical exponents ds/z , d_F/z , and $1/z$ for size, fatalities, and geographic extent, respectively. The distributions of the scaling variables are likewise expected

to scale simply

$$P(S) \sim S^{-\tau} \quad (4)$$

$$P(F) \sim F^{-\tau'} \quad (5)$$

$$P(L) \sim L^{-\nu} \quad (6)$$

$$P(T) \sim T^{-\alpha} \quad (7)$$

The relations in Eqs 1–7 provide the basis for a scaling hypothesis of armed conflict that we test empirically.

If conflict avalanches grow in time, space, and magnitude in a self-similar manner, we expect that the dynamical exponents should be related to the power law exponents in a consistent way. To measure the dynamical exponents, we directly compare the scaling variables to determine $d_S/z = 2.0 \pm 0.3$, $d_F/z = 2.5 \pm 0.3$, and $1/z = 0.8 \pm 0.1$ (SI Section C). Then, we construct the distributions of the scaling variables (Fig. 2B), and we find via a standard procedure that they are statistically indistinguishable from power laws [18]. The corresponding exponents appear in Fig. 2C, where for the highlighted case of $a = 128$ days, we find $\tau = 1.96 \pm 0.03$, $\tau' = 1.65 \pm 0.08$, $\alpha = 2.44 \pm 0.13$, and $\nu = 2.78 \pm 0.21$. In a self-consistent framework, the measured exponents must satisfy the relations

$$\alpha - 1 = d_S(\tau - 1)/z = d_F(\tau' - 1)/z = (\nu - 1)/z. \quad (8)$$

These relations are satisfied within 90% bootstrap error intervals. Thus, the various features of conflict including, perhaps surprisingly, L are unified in a self-consistent fashion given a simple scaling description.

Self-similarity also predicts that the average evolution of each scaling variable within an avalanche approaches a universal profile at large scales. The normalized trajectories of size $\int_0^t \langle s(t', T)/S \rangle dt'$, fatalities $\int_0^t \langle f(t', T)/F \rangle dt'$, and geographic extent $\langle l(t, T)/L \rangle$ give the cumulative fraction of total events or extent by scaled time t/T (insets in Fig. 3). For sizes and fatalities, at least one event occurs at $t = 0$ and $t = T$ by construction, so we must account for a $1/S$ “lattice” bias to obtain a collapse (SI Section E). We find across avalanches with duration $T > a$ that the cumulative profiles overlap. Furthermore, we collapse the rate profiles (without integration or normalization) to measure the dynamical exponents, and these are consistent with the scaling relations in Eq 8 (SI Section E). This overlap between the temporal profiles indicates that the dynamics of long conflicts may be dominated by a scale-invariant process as is consistent with a scaling framework.

Notably, the statistical structure encoded in the exponent relations in Eq 8 and temporal profiles is largely preserved as we change the separation time a . In Fig. 2, we show that the exponents stay close to their values in the highlighted example over an order of magnitude of $16 \leq a \leq 256$ days, and in Fig. 3 the average temporal profiles hardly change across the matching range of

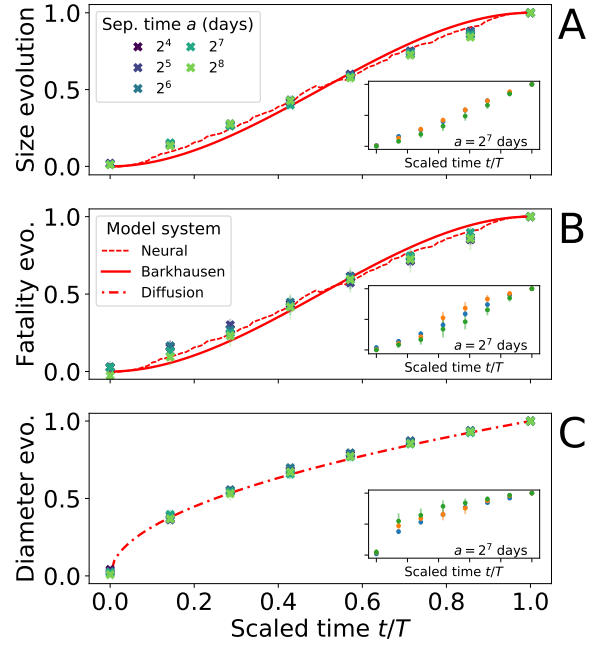


FIG. 3. Temporal evolution measured by cumulative fraction of (A) sizes as number of reports, (B) fatalities, and (C) geographic extent along scaled time t/T . Profiles are averaged over all avalanches with duration exceeding the separation time a . Stochasticity of lattice correction for fatalities can induce small negative values at $t = 0$ (SI Section E). We compare conflicts with the normalized trajectory for experimental neural avalanches (dashed red line, $K > 10^3$ [16]), Barkhausen noise $\int_0^{t/T} V(t') dt' = 3(t/T)^2 - 2(t/T)^3$ (solid red line [19]), and diffusive growth $l(t/T) = (t/T)^{1/2}$ (dot-dashed red line [23]). (insets) For separation time $a = 128$ days, we show that average profiles when binned by conflict duration overlap. Bins are for conflicts of durations (blue) 2^7 – 2^9 days, (orange) 2^9 – 2^{11} days, and (green) 2^{11} – 2^{13} days. Error bars represent 90% bootstrapped confidence intervals of the means.

a. In physical systems near a critical point, symmetries under rescaling are expected. In our case, increasing a does not exactly correspond to rescaling time but rather groups together events that are increasingly further apart into the same avalanche. Yet remarkably, we find that doubling a is statistically analogous to scaling T in that it largely preserves the exponents and temporal profiles across timescales from weeks to years, a result that reflects self-similarity in the timing of conflict events [3].

The temporal profiles hint at the underlying dynamics generating conflict avalanches. For comparison, we show profiles of canonical systems with self-similar avalanches like Barkhausen noise and an example of a neural culture. These tend to accelerate in the middle whereas average size and fatality profiles for conflict avalanches tend to evolve at a more linear pace. Flat profiles can indicate dissipative effects that suppress large events as with demagnetizing fields in Barkhausen noise [19]. Yet, flattening is also a feature of both subcritical and super-

	Size τ	Fatalities τ'	Diameter ν	Duration α	S vs. T d_S/z	F vs. T d_F/z	L vs. T $1/z$
Battles	1.96	1.65	2.78	2.44	2.0	2.5	0.78
Forest fires 2D	2.14			1.27	1.89		0.96
Forest fires 5D	2.45			1.89	1.98		0.62
Percolation 2D	2.05				1.68		
Barkhausen mean field	3/2			2	4		1/2
Neural	2.10			2.86	1.85		
Wars		1.53					

TABLE I. Scaling exponents for Battles conflict avalanches with those for physical, biological, and social systems. Critical exponents are shown for forest fires in 2D and near the upper critical dimension [25], percolation [25], Barkhausen noise mean-field theory, *i.e.* the random field Ising model [26], and experimental neural avalanches [17]. For comparison, we show the fatality exponent for interstate wars—defined sociopolitically in contrast to our conflict avalanches—from 1823–2003 [5]. The exponent d_S corresponds to the conventional choice of exponents $1/\sigma\nu$ for fractal dimension. Where the exponent error intervals overlap with those of Battles, we color the box light blue. Where exponents are notably similar but significantly different, we outline the box.

critical cascades that spontaneously end—though such profiles will fail to collapse [20, 21]. Thus, the mapping between dynamics and profile is many-to-one, but we can rule out analogues of properties that, for example, generate asymmetric profiles such as eddy currents in magnetic materials [19], certain networks like in disassociated neural cultures [15], or variations in birth-death processes [21]. In contrast, we find that spatial extent grows in a strongly nonlinear and asymmetric fashion as shown in Fig. 3C. This profile is closely described by the average linear extent of a convex hull of planar Brownian walkers [22, 23], perhaps related to properties of generalized diffusion models used to describe other conflict data sets [24]. More generally, these profiles are compatible with Markovian cascades on networks indicating that such dynamics may come to dominate in long conflict avalanches.

Beyond temporal profiles, the measured exponents indicate how the spread of armed conflict is comparable to physical, biological, and social systems in Table I. In agreement with our observations with temporal profiles, armed conflict shows differences with the cascade processes listed. Of particular note is the self-organized critical forest fire (FF) model that shows strong disagreement with duration exponent α both far from mean-field and close to the upper critical dimension. This model is oft-cited in the context of human conflict [6, 8]. In comparison, our measured exponents are similar to those for percolation in 2D that lie just beyond our confidence bounds. Such similarity hints that the spread of armed conflict is comparable to growth processes on networks at

the percolation threshold as appears to be the case with neural avalanches in zebrafish [17]. We note that the scaling of S vs. T is nearly quadratic for most of the listed processes, reflecting the fact that events happen faster in larger avalanches, one way of distinguishing small conflicts from larger ones early on. Furthermore, the relation between time and spatial extent L vs. T means that Battles, like forest fires, are space-filling: $d_S \gtrsim 2$ on the approximately 2D surface of the Earth. Thus, in this way we can use scaling exponents to systematically compare armed conflict with other physical processes relying on the formalism of universality classes from physics.

The emergence of these large-scale symmetries is extraordinary. Such remarkable regularity presents an opportunity for prediction [27]. In particular, knowledge of the temporal profiles suggests one way of extrapolating from the beginning of an ongoing conflict the potential human cost of the rest of the conflict before it ends. Scaling relations could be used to estimate missing data points like fatalities (which are especially difficult to measure), to detect anomalous statistics, or to help assess risk for nearby regions by showing how geographic extent scales with duration. These statistics are extracted from clusters of conflict events generated from simple physical scales, providing a well-defined, quantitative, and straightforwardly measured procedure as a complement to sociopolitical definitions of wars. Taken together, our results reveal a unified framework for conflict growth in which physical space and time scales constrain a social phenomenon. Universality and scaling laws have been found in a variety of social systems [28, 29], suggesting self-similarity and the renormalization group as means to understanding how physical constraints translate into emergent patterns at large scales. In this wider context, our findings hint at the intriguing possibility that emergent regularities reflect underlying physical principles that shape the evolution of armed conflict.

We thank Veit Elser, Guru Khalsa, Sid Redner, and Simon Dedeo for helpful discussion. We acknowledge an NSF GRFP under grant no. DGE-1650441 (EDL), NSF no. 0904863 (JCF & DCK), a St. Andrews Foundation grant of no. 13337 (EDL, JCF & DCK), a John Templeton Foundation grant of no. 60501 (JCF & DCK), the Proteus Foundation (JCF), and the Bengier Foundation (JCF).

- [1] L. F. Richardson. Frequency of Occurrence of Wars and other Fatal Quarrels. *Nature*, 148(3759):598–598, November 1941.
- [2] A. Clauset, M. Young, and K. S. Gleditsch. On the Frequency of Severe Terrorist Events. *Journal of Conflict Resolution*, 51(1):58–87, February 2007.
- [3] S. Picoli, M. del Castillo-Mussot, H. V. Ribeiro, E. K. Lenzi, and R. S. Mendes. Universal bursty behaviour in

human violent conflicts. *Sci Rep*, 4(1):4773, April 2014.

[4] C. S. Gillespie. Estimating the number of casualties in the American Indian war: A Bayesian analysis using the power law distribution. *Ann. Appl. Stat.* 11(4):2357–2374, June 2017.

[5] A. Clauset. Trends and fluctuations in the severity of interstate wars. *Science Advances*, 4(eaao3580):1–9, February 2018.

[6] L. E. Cederman. Modeling the size of wars: From billiard balls to sandpiles. *Am Political Sci Rev*, 97(1):135–150, February 2003.

[7] J. C. Bohorquez, S. Gourley, A. R. Dixon, M. S., and N. F. Johnson. Common ecology quantifies human insurgency. *Nature*, 462(7275):911–914, December 2009.

[8] D. C. Roberts and D. L. Turcotte. Fractality and self-organized criticality of wars. *Fractals*, 6(4): 351–357, September 1998.

[9] J. Cardy. *Scaling and Renormalization in Statistical Physics*. Cambridge Lecture Notes in Physics. Cambridge University Press, 1996.

[10] J. J. Binney, N. J. Dowrick, A. J. Fisher, and M. E. J. Newman. *The Theory of Critical Phenomena*. An Introduction to the Renormalization Group. Oxford University Press, Oxford, 1993.

[11] J. P. Sethna, K. A. Dahmen, and C. R. Myers. Crackling noise. *Nature*, 410(6825):242–250, March 2001.

[12] J. L. Cardy. Finite Size Scaling, Vol. 2, 1988.

[13] B. C. Daniels, D. C. Krakauer, and J. C. Flack. Control of finite critical behaviour in a small-scale social system. *Nat Comms*, 8:14301–8, February 2017.

[14] C. Raleigh, A. Linke, H. Hegre, and J. Karlsen. Introducing ACLED: An Armed Conflict Location and Event Dataset. *JPR*, 47(5):651–660, August 2010.

[15] N. Friedman, S. Ito, B. A. W. Brinkman, M. Shimono, R. E. L. DeVille, K. A. Dahmen, J. M. Beggs, and T. C. Butler. Universal Critical Dynamics in High Resolution Neuronal Avalanche Data. *Phys Rev Lett*, 108(20):208102-1–5, May 2012.

[16] N. M. Timme, N. J. Marshall, N. Bennett, M. Ripp, E. Lautzenhisler, and J. M. Beggs. Criticality Maximizes Complexity in Neural Tissue. *Front Physiol*, 7(163):e85777–19, September 2016.

[17] A. Ponce-Alvarez, A. Jouary, M. Privat, G. Deco, and G. Sumbre. Whole-Brain Neuronal Activity Displays Crackling Noise Dynamics. *Neuron*, 100:1446–1459, December 2018.

[18] A. Clauset, C. R. Shalizi, and M. E. J. Newman. Power-Law Distributions in Empirical Data. *SIAM Review*, 51(4):661–703, November 2009.

[19] S. Papanikolaou, F. Bohn, R. L. Sommer, G. Durin, S. Zapperi, and J. P. Sethna. Universality beyond power laws and the average avalanche shape. *Nature Physics*, 7(4):316–320, April 2011.

[20] J. Hindes and I. B. Schwartz. Epidemic Extinction and Control in Heterogeneous Networks. *Phys Rev Lett*, 117(2):028302-1–5, July 2016.

[21] J. P. Gleeson and R. Durrett. Temporal profiles of avalanches on networks. *Nat Comms*, 8(1):1–12, October 2017.

[22] M. Kot, M A Lewis, and P van den Driessche. Dispersal Data and the Spread of Invading Organisms. *Ecology*, 77(7):20272042, 1996.

[23] J. Randon-Furling, S. N. Majumdar, and A. Comtet. Convex Hull of N Planar Brownian Motions: Exact Results and an Application to Ecology. *Phys Rev Lett*, 103(14):140602-1–4, October 2009.

[24] A. Zammit-Mangion, M. Dewar, V. Kardirkamanathan, and G. Sanguinetti. Point Process Modelling of the Afghan War Diary. *PNAS*, 109(31):12414–12419, June 2012.

[25] S. Clar, B. Drossel, and F. Schwabl. Scaling laws and simulation results for the self-organized critical forest-fire model. *Phys Rev E*, 50(2):1009–1018, August 1994.

[26] O. Perković, K. A. Dahmen, and J. P. Sethna. Disorder-induced critical phenomena in hysteresis: Numerical scaling in three and higher dimensions. *Phys Rev B*, 59(9):6106–6119, March 1999.

[27] M. Spagat, N. F. Johnson, and S. V. Weezel. Fundamental patterns and predictions of event size distributions in modern wars and terrorist campaigns. *PLoS ONE* 13(10):e0204639-1–13, October 2018.

[28] S. Fortunato, C. Castellano. Scaling and Universality in Proportional Elections. *Phys Rev Lett*, 99(13):138701-1–4, September 2007.

[29] L. M. A. Bettencourt, J. Lobo, D. Helbing, C. Kühnert, G. B. West. Growth, Innovation, Scaling, and the Pace of Life in Cities. *PNAS* 104(17):7301–7306, April 2007.